Creep and Shrinkage Behavior of Improved Ultrathin Polymeric Films

TAKUJI HIGASHIOJI,* BHARAT BHUSHAN

Nanotribology Laboratory for Information Storage and MEMS/NEMS, Department of Mechanical Engineering, The Ohio State University, 206 West 18th Avenue, Columbus, Ohio 43210

ABSTRACT: Long-term creep-deformation and shrinkage characteristics of improved ultrathin polymeric films for magnetic tapes are presented. These films include poly-(ethylene terephthalate) (PET), poly(ethylene naphthalate) (PEN), and aromatic poly-amide (ARAMID). PET film is currently the standard substrate used for magnetic tapes, and thinner tensilized-type PET, PEN, and ARAMID have recently been used as alternate substrates with improved material properties. The thickness of the films ranges from 6.2 to 4.8 μm. More dimensional stability is required for advanced magnetic tapes, and the study of creep and shrinkage behavior is important for estimating the dimensional stability. Creep measurements were performed on all available substrates at 25, 40, and 55°C for 100 h. Based on these data, master curves were generated using time–temperature superposition to predict dimensional stability after several years. The amount of creep deformation is considerably smaller for ARAMID and tensilized-type PET than for PEN, although Standard PET shows the largest amount of creep. In addition, creep measurements under high humidity also show similar trends. Shrinkage measurements at 55°C for 100 h show that the shrinkage of ARAMID is lower than that of PET and PEN. The relationship between the polymeric structure and dimensional stability are also discussed. Based on the creep and shrinkage behavior, ARAMID and tensilized-type PET seem to be suitable for advanced magnetic tapes. © 2002 Wiley Periodicals, Inc. J Appl Polym Sci 84: 1477–1498, 2002; DOI 10.1002/app.10012

Key words: viscoelastic properties; creep; films

INTRODUCTION

Poly(ethylene terephthalate) (PET) is currently the most widely used polymeric substrate material for magnetic recording tapes.[1] Thinner substrates and higher areal densities (track density × linear density) are required to meet the demand for advanced magnetic storage devices with high volumetric densities, especially for computer data-storage tapes. For higher areal densities, a substrate with higher mechanical and higher dimensional stability under various environmental conditions is required. For high densities, lateral contraction of the substrates due to thermal, hygroscopic, viscoelastic (creep), and shrinkage effects must be minimal during storage on a reel and used in a drive.[1] The study of creep and shrinkage behavior is important for estimating the dimensional stability. To minimize stretching and damage during use, the substrates should be a high-modulus and high-strength material with low creep and shrinkage characteristics. It should be noted that, in a linear tape drive, longitudinal

deformations could be accommodated by a change in a clocking speed, whereas, in a rotary drive, both longitudinal and transverse deformations are important. As the tape is unwound and goes over the head, elastic and viscoelastic recovery is important.[1]

Viscoelasticity, or creep, refers to the combined elastic and viscous deformation of a substrate when an external stress is applied. This includes both recoverable and nonrecoverable deformation after removing external stress. Shrinkage occurs when residual stresses present in the substrate are relieved at elevated temperature, and, thus, shrinkage is a nonrecoverable deformation process. If a substrate of a magnetic tape shrinks or deforms viscoelastically, then the head cannot read information stored on the tape. Various long-term reliability problems including uneven tape-stack profiles (or hardbands), mechanical print-through, instantaneous speed variations, and tape stagger problems can all be related to the viscoelastic property of substrates.[1] To minimize these reliability problems, it is not only important to minimize creep strain, but the rate of increase of total strain also needs to be kept to a minimum to prevent stress relaxation in a wound reel.

Realistic dimensional stability of tape-pack stresses is an important issue. To our knowledge, however, effective measurements have not been made to analyze the deformation in response to tape-pack stresses. In the present study, simplified model tests were conducted, and basic data were collected with regard to the dimensional stability of tape substrates. Tape substrates were placed under tension in the tape direction. These data are needed to predict deformations in a tape pack. We focused on the irreversible properties, which include creep behavior in a tape direction, shrinkage, and creep recovery. Measurements of reversible properties, like thermal and hygroscopic expansion coefficients, could be items for following studies.

Alternate substrates considered include thinner tensilized-type PET, poly(ethylene naphthalate) (PEN), and aromatic polyamide (ARAMID). Weick and Bhushan presented viscoelastic, shrinkage, and mechanical properties of some alternate substrates[1-4] and magnetic tapes.[1,3,5,6] Substrates of magnetic tapes have recently been improved substantially. The main objective of this study was to measure the viscoelastic (creep compliance) and shrinkage characteristics of improved ultrathin polymeric films that are either being used or developed for magnetic tape sub-strates for ultrahigh recording applications. Experiments were carried out at temperatures ranging from ambient to 55°C, which is the upper design limit for magnetic tapes. The upper-limit temperature was 50°C in previous research,[2] but the temperature has recently been increased for the demand of advanced magnetic tape systems. From these measurements, the rate of creep was determined, and lateral contraction of the substrates due to Poisson effects was calculated. Master curves were generated using time–temperature superposition to predict long-term creep behavior. Creep-recovery characteristics were also evaluated. In addition, creep deformation under a severe condition with high temperature and high humidity was measured to estimate the effect of humidity. Shrinkage measurements were made to determine the extent of nonrecoverable deformation undergone by the materials at elevated temperatures, and both creep and shrinkage behavior were related to the structural characteristics of each polymer.

EXPERIMENTAL

Test Apparatus

Creep and shrinkage characteristics of polymeric films were evaluated using the test apparatus shown in Figure 1. Up to four samples were tested simultaneously using this apparatus, and creep properties at elevated temperature and/or humidity levels could be obtained by performing experiments in an environmental chamber. The apparatus consisted of four load arms, and polymeric films were fixed at the end of each arm and aligned with a straight edge. A linear variable differential transformer (LVDT) was connected to the other end to measure deflection of the load arm due to creep deformation of the film sample, and the output was recorded on a personal computer (PC). The load was applied on the load arm remotely using a pneumatically controlled mechanism, since the apparatus was placed in an environmental chamber. As shown in Figure 1, weights were placed on top of rectangular pieces positioned around each load arm. These rectangular pieces were suspended from a single crossbar, and lowering or raising this crossbar using an air cylinder controlled the loads imposed on the load arm.

Test Samples

Table I provides a list of the polymeric films examined in this study along with their thicknesses,
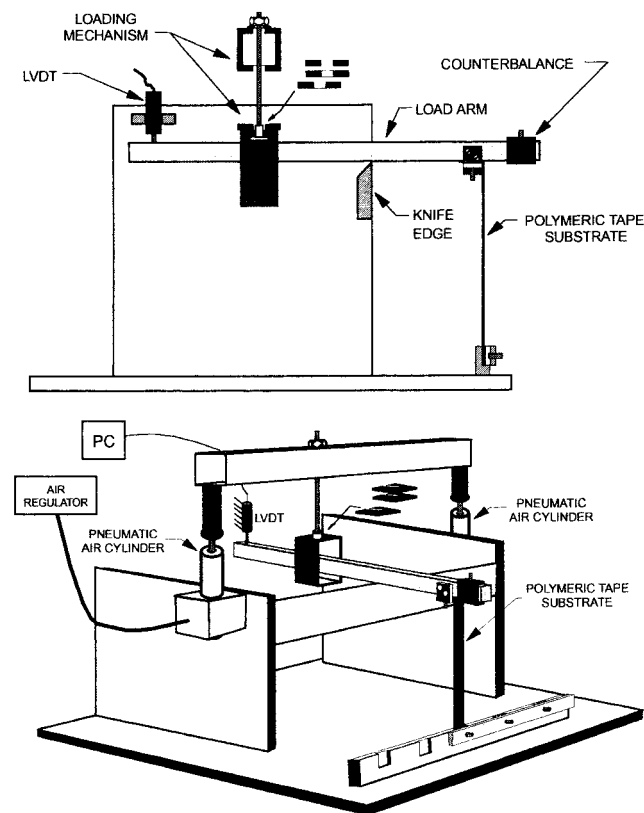
Figure 1 Experimental apparatus for evaluating creep and shrinkage behavior of polymeric films.

mechanical properties, and heat-shrinkage data. The samples are available as commercial films. PET films include three kinds of films: Standard PET, Tensilized PET, and Supertensilized PET. A 14-μm-thick Standard PET film is the typical sub-

strate used for videocassette recorder (VCR) tapes. Standard PET is drawn biaxially by the ratio of approximately four times in both the machine direction (MD) and the transverse direction (TD) during processing. Thinner tensilized-type PET films, which include additional drawn Tensilized PET and more additional drawn Supertensilized PET, are tensilized in an MD and have a 6.1-μm thickness. The tensilized-type PET films are used for advanced magnetic tapes, especially computer data-storage tapes. Similarly, PEN films have 6.2-μm thickness and include three kinds of films: Standard PEN, Tensilized PEN, and Supertensilized PEN. PEN films have begun to be used as substrates for advanced magnetic tapes, especially long-play videotapes and computer data-storage tapes. Both PET and PEN films are manufactured by a biaxial drawing process. In general, the Young's modulus, F-5 value, and heat-shrinkage shown in Table I represent the data of processed films, which include crystalline and amorphous states. For PET and PEN, more tensilization leads to higher values of the modulus and strength and more shrinkage. On the other hand, ARAMID film is manufactured using a solution-casting process and then drawn slightly using a drawing process. ARAMID has a 4.8-μm thickness which is used for advanced magnetic tapes. The symbols in Table I are used throughout the article.

The polymeric unit structure of substrates is illustrated in Figure 2. PET and PEN have identical hydrocarbon backbones, indicative of polyester materials. PET contains a single benzene ring in each repeating unit, whereas PEN contains a

Table I   List of Substrates for Magnetic Tapes

Sample	Symbol	Thickness (μm)	Young's Modulus[a] MD/TD (GPa)	F-5 Value[a,b] MD/TD (MPa)	Heat Shrinkage[a,c] MD/TD (%)
Standard PET[d]	Standard PET	14.0	4.4/6.2	113/143	0.7/0.3
Tensilized PET	T-PET	6.1	7.2/4.5	180/108	1.2/0.2
Supertensilized PET	ST-PET	6.1	8.5/5.2	229/121	2.4/−0.2
Standard PEN[d]	Standard PEN	6.2	7.0/7.3	173/202	0.5/0.3
Tensilized PEN	T-PEN	6.2	8.0/6.5	184/161	0.3/0.2
Supertensilized PEN	ST-PEN	6.2	9.0/6.0	217/139	0.3/0.2
ARAMID[d]	ARAMID	4.8	19.3/11.5	590/390	0.0/0.0

[a] The values were provided by the suppliers.
[b] F-5 value represents strength at strain of 5%.
[c] Shrinkage was measured after 30 min at 105°C.
[d] The glass transition temperature for PET, PEN, and ARAMID films are typically 105, 125, and 280°C, respectively.

naphthalene ring that is slightly more rigid. But naphthalene groups have high mobility from ambient temperature to 60°C.[7] PET has more crystalline phases than has PEN. ARAMID has rigid rod-like structures that exhibit a high degree of orientation. In addition, ARAMID contains amide groups with intermolecular hydrogen bonds that are stronger than are the intermolecular interaction of PET and PEN. As a result, ARAMID enables the formulation of high-strength, high-modulus films.

Experimental Procedure

For both creep and shrinkage measurements, the samples were cut with a paper cutter into 190-mm-long × 12.7-mm (1/2 in.)-wide strips to accommodate the creep apparatus. The resulting strain was determined by measuring the change in length of the samples relative to their original length. The chamber was opened and the samples were fastened between the load arms and the base of the creep tester. Prior to attaching the samples, the environmental chamber was turned on to stabilize the temperature and humidity in the chamber and to allow the creep tester to be conditioned for 1 h.

For the creep experiments, the samples were conditioned at a preset temperature without a load for 1 h after attaching. Next, a preload of 0.5

Table II   Test Conditions

Creep measurements
    Duration of measurements: 100 h
    Applied external stress: 7.0 MPa
    Temperature (relative humidity):
        25°C (50–60% RH: uncontrolled)
        40°C (15–25% RH: uncontrolled)
        55°C (5–10% RH: uncontrolled)
        55°C (80% RH)

Shrinkage measurements
    Duration of measurements: 100 h
    Applied external stress: 0.5 MPa
    Temperature (relative humidity):
        55°C (5–10% RH: uncontrolled)

MPa was applied to the film samples by adjusting the counterbalance weight on the load arm, and then the samples were conditioned for stabilization in an environmental condition. During this stabilization period of typically 2 h, the output signals were monitored until they were steady. The conditioning procedure, for instance, has the effect on the creep behavior that the sample has lost its long-term memory and currently remembers loads applied in its immediate past history.[8] The test conditions are summarized in Table II. Since 55°C is the upper design limit for magnetic tapes, creep measurements were performed at 55, 40, and 25°C for a duration of 100 h. Humidity was not controlled, and relative humidity (RH) was 5–10%, 15–25%, and 50–60% at 55, 40, and 25°C, respectively. In addition, creep deformation under a severe condition was measured at 55°C and a controlled 80% RH. The constant external stress of 7.0 MPa was applied to the samples using the pneumatic control mechanism. This stress was chosen as the general stress in a tape drive and has been shown to keep the creep experiments in the linear viscoelastic regime.[1] In a previous research,[2] preliminary experiments at higher stresses for PET, PEN, and ARAMID films also showed that nonlinear viscoelastic behavior did not occur. Ward and Hadley[8] also described that, in the linear viscoelastic region, strains were unlikely to exceed 1%. Tsou et al.[9] reported that a nonlinear viscoelastic response was observed at strains exceeding 0.8% in some polymeric films including PET. Creep measurements were made in an MD along with a tape direction, since stress is applied along the tape direction during operation and in a wound reel of a magnetic tape. It was confirmed that an MD corre-
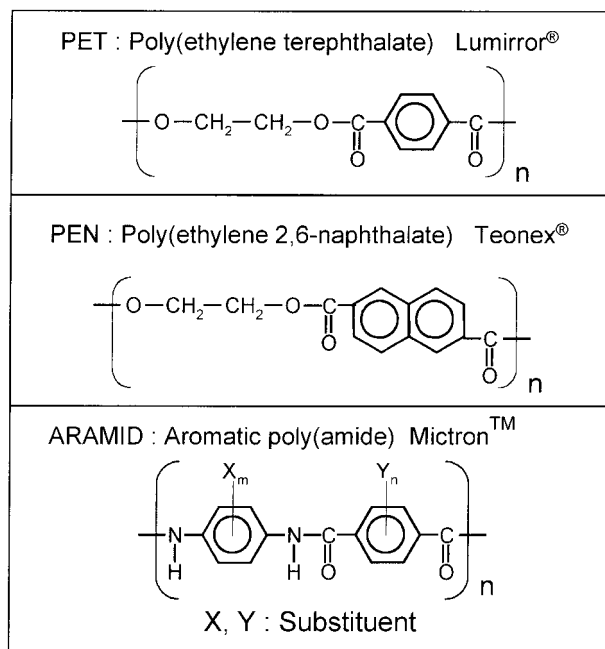

Figure 2   Chemical unit structures of polymeric films.
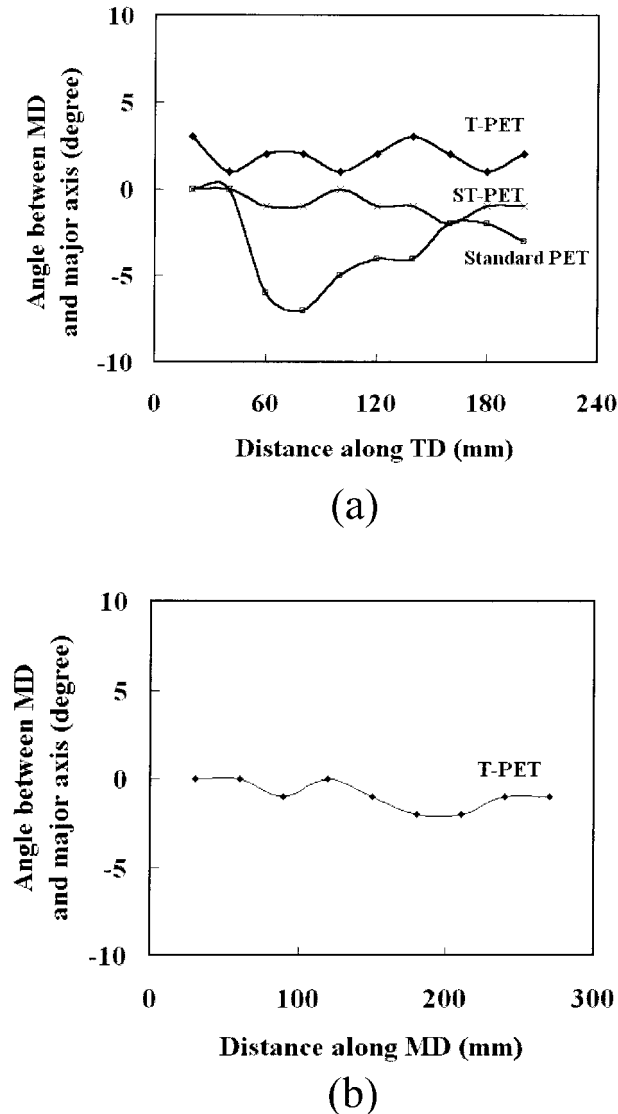
(a)

(b)

Figure 3 Orientation of the optical major axis with respect to the MD of PET films (a) along TD and (b) MD.

sponds to the direction of orientation of crystals in biaxial films using a cross-polarizer in which optical axes show the extinction of light. Two linear polarizing films of 2-in. square (Tech Spec^{TM} Quality J43-781, Edmund Scientific, Tonowanda, NY) were used. As examples, Figure 3 shows the orientation of the major axis with respect to the MD of PET films. The difference between the major axis and the MD is below ±5°.

For the first hour, the sampling rate for the data-acquisition system was set to 12.5 samples/s per load arm, and 25 data points acquired into memory were averaged for each data point recorded on the computer hard disk. After 1 h, the

sampling rate was slowed to 0.25 samples/s with the same averaging scheme. Creep characteristics were measured for an additional 99 h. At the end of the 100-h measurements, the sampling rate was once again increased to 12.5 samples/s per load arm, and the samples were pneumatically unloaded. Recovery characteristics experiments were then conducted at the lower sampling rate for 10 h.

Shrinkage experiments were also performed at 55°C and 5–10% RH for 100 h, and a minimal applied stress of 0.5 MPa was used to hold the samples in place without causing any substantial creep of samples after they were fastened to the grips. The sampling rate of 0.25 samples/s per load arm was used, and 25 data acquired into the memory were averaged for each data point recorded on the computer hard disk. Shrinkage measurements were made both in an MD and a TD.

Data Reduction Method

During an experiment, the LVDT connected to each load arm detects the change in length of each polymeric film. This change in length is, in general, a nonlinear function of time and temperature. The amount of strain can be calculated by normalizing the change in length of the film samples with respect to the original length. Creep compliance can then be obtained by dividing the time-dependent strain by the constant applied external stress:

$$\varepsilon(t) = \frac{\Delta l(t)}{l_0} \tag{1}$$

$$D(t) = \frac{\varepsilon(t)}{\sigma_0} = \frac{\Delta l(t)}{\sigma_0 l_0} \tag{2}$$

where $\varepsilon(t)$ is the amount of strain which the polymeric film is subjected to; $\Delta l(t)$, the change in length of the polymeric film as a function of time; l_0, the original length of the polymeric film; $D(t)$, the creep compliance of the polymeric film as a function of time; and σ_0, the constant applied external stress. In shrinkage measurements, the strain $\varepsilon(t)$ represents the amount of shrinkage. If the films shrink, the strain has a negative value, whereas the strain has a positive value if the films expand.
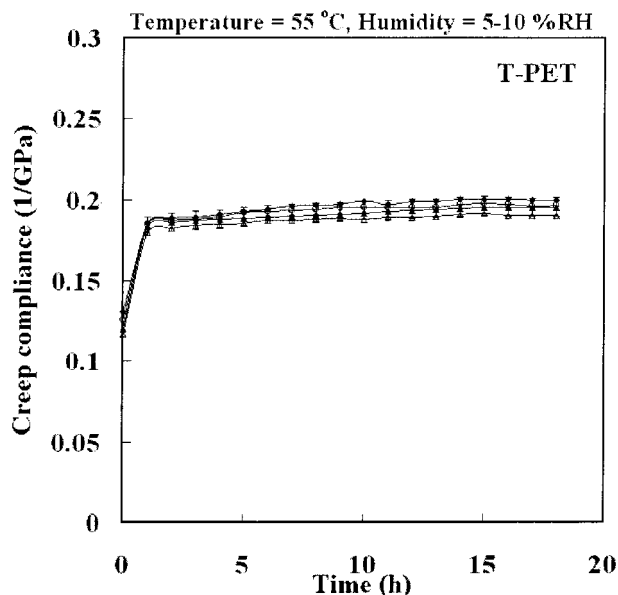
Figure 4 Reproducibility of creep-compliance measurements.

RESULTS AND DISCUSSION

Creep-compliance Measurements

Creep experiments were performed at 55, 40, and 25°C temperature levels. A level of 55°C was selected as the typical upper limit used for magnetic tapes, because the motivation of this study was to characterize improved alternate substrates for advanced magnetic tapes. Reproducibility of creep data will be first presented, followed by detailed creep-compliance measurements, creep-velocity characteristics obtained by differentiating the creep data, and temperature-dependent creep compliance. Lateral contraction calculations based on Poisson effects will also be discussed.

As an example of the reproducibility of creep data, Tensilized PET film measured at four load arms is shown in Figure 4. The error vertical bars inserted in the data curves mean an error of less than 3% from the average data. The error can be regarded as tolerance, and it is evident that creep data measured using the creep apparatus in this study would have high reliability.

Creep-compliance measurements for polymeric films are shown in Figure 5 for 55, 40, and 25°C. The data sets are plotted on a linear scale on the left of Figure 5 and on a log–log scale on the right of Figure 5. The measured direction is an MD along a tape direction. For all the samples, it can

be seen that an initial deformation occurs instantaneously due to the elastic and short-term viscoelastic behavior of the materials. The amount of creep compliance gradually increases throughout the experiment due to the viscoelastic contribution. Table III summarizes the creep-compliance data after 0.01, 0.1, 1, 10, and 100 h and the increment from 0.01 to 100 h.

ARAMID and tensilized-type PET, which includes T-PET and ST-PET, show a lower increase of deformation at all the temperatures, whereas PEN and Standard PET have a larger increase. On comparison of creep compliance, ARAMID shows the lowest creep. The total amount of creep compliance is considerably smaller for tensilized-type PET than for PEN at all temperature levels, and Standard PET shows the largest amount of creep. As an example, creep compliance for a 55°C temperature level is described. ARAMID has the lowest total amount of 0.101 GPa^{-1}, and the lowest increment of 0.008 GPa^{-1} from 0.01 to 100 h. For tensilized-type PET, the total amount of about 0.19 GPa^{-1} is still less, and the increment of about 0.02 GPa^{-1} from 0.01 to 100 h is also lower. In contrast to the results of ARAMID and tensilized-type PET, PEN shows a larger total amount of about 0.24–0.30 GPa^{-1} and a larger increment of about 0.7 GPa^{-1}. Standard PET has the largest total amount and increment. It should be noted that the creep property of thinner tensilized-type PET films is more improved and different from that of thick Standard PET. Besides, the results of 55°C are likely to correspond with the previous research[1,2] for PEN and thick Standard PET. The larger creep deformation at 55°C for PEN could be attributed to the high mobility of PEN molecules at this temperature.[7] A detailed consideration on the polymeric structure is discussed in the following section. In addition, more tensilization is likely to result in less creep for both PET and PEN, which is obvious for PET. Furthermore, creep-compliance measurements at 40 and 25°C show similar trends, although the total amount at 40 and 25°C is lower than at 55°C.

From the slopes of the creep-compliance curves in Figure 5, the rate of creep can be determined. The first derivative of the creep curves at a 55°C temperature level were calculated and are plotted in Figure 6. These data indicate creep velocity. Creep velocity decreases for all polymeric films and approaches zero. These results imply that creep deformation could reach a steady state in the long term. Creep-velocity measurements show
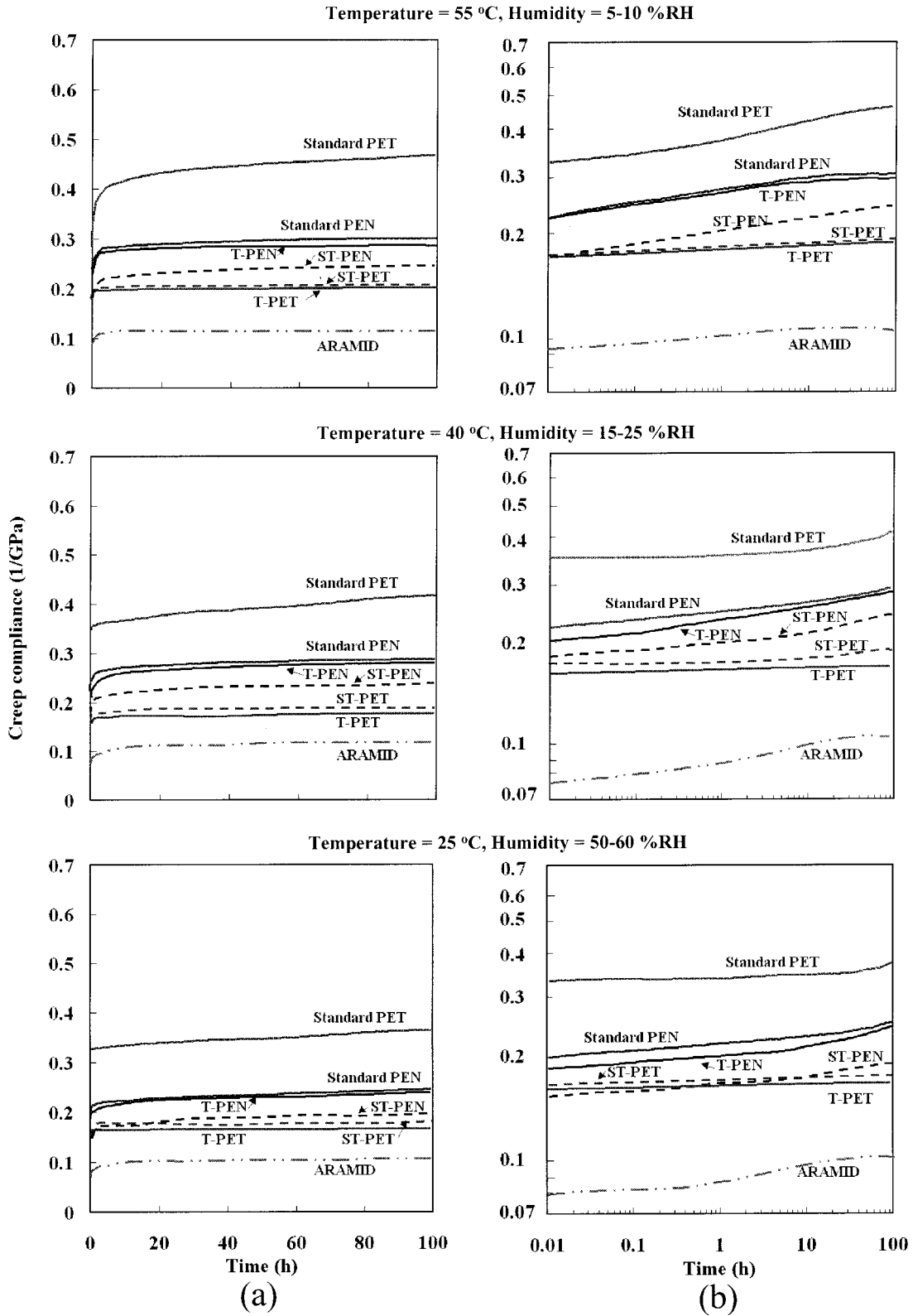
Figure 5 Creep-compliance measurements for polymeric films at 55, 40, and 25°C. Plotted on (a) linear axes and (b) log–log axes.

Table III   Creep Compliance Data at Various Temperatures

	Creep Compliance (1/GPa; 55°C, 5–10% RH)						
Sample	0.01 h	0.1 h	1 h	10 h	100 h	110 h[a]	100 h − 0.01 h[b]
Standard PET	0.320	0.339	0.369	0.420	0.470	0.141	0.150
T-PET	0.170	0.177	0.184	0.194	0.193	0.000	0.023
ST-PET	0.173	0.179	0.187	0.199	0.189	0.000	0.016
Standard PEN	0.222	0.244	0.267	0.290	0.296	0.036	0.074
T-PEN	0.222	0.244	0.264	0.282	0.285	0.044	0.063
ST-PEN	0.173	0.188	0.204	0.223	0.244	0.048	0.071
ARAMID	0.093	0.097	0.102	0.109	0.101	0.018	0.008

	Creep Compliance (1/GPa; 40°C, 15–25% RH)						
Sample	0.01 h	0.1 h	1 h	10 h	100 h	110 h[a]	100 h − 0.01 h[b]
Standard PET	0.350	0.350	0.356	0.366	0.414	0.100	0.064
T-PET	0.165	0.165	0.168	0.167	0.177	0.018	0.012
ST-PET	0.174	0.174	0.176	0.180	0.194	0.018	0.020
Standard PEN	0.223	0.233	0.247	0.264	0.289	0.041	0.066
T-PEN	0.200	0.214	0.225	0.247	0.269	0.061	0.069
ST-PEN	0.182	0.191	0.200	0.213	0.234	0.038	0.052
ARAMID	0.078	0.082	0.086	0.099	0.107	0.017	0.029

	Creep Compliance (1/GPa; 25°C, 50–60% RH)						
Sample	0.01 h	0.1 h	1 h	10 h	100 h	110 h[a]	100 h − 0.01 h[b]
Standard PET	0.324	0.324	0.324	0.330	0.366	0.055	0.042
T-PET	0.161	0.161	0.161	0.161	0.170	0.017	0.009
ST-PET	0.167	0.167	0.167	0.169	0.176	0.005	0.009
Standard PEN	0.195	0.203	0.211	0.220	0.246	0.034	0.051
T-PEN	0.180	0.188	0.196	0.210	0.239	0.025	0.059
ST-PEN	0.150	0.155	0.162	0.168	0.183	0.019	0.033
ARAMID	0.078	0.080	0.086	0.096	0.102	0.011	0.024

[a] 10 h after removing external applied stress.
[b] Increment of creep compliance from 0.01 to 100 h.

ARAMID has the lowest rate of creep throughout the experiments, followed by tensilized-type PET, PEN, and Standard PET. This order is similar to the creep-compliance measurements.

Additional information can be extracted from the slopes of the creep-velocity curves in Figure 6. These slopes indicate acceleration or deceleration during the creep process. Typically, the materials show a decreasing creep velocity and a negative slope, which indicates deceleration during the creep process. In a previous research,[2] it was observed that ARAMID continued to creep at the same rate without a change in velocity. In this study, however, the slope of the creep-velocity curve for ARAMID decreases throughout the measurement. This means that ARAMID was also improved substantially compared to the previous material. In addition, creep velocity is likely to be related to the permanent deformation in a recovery test.[1] A detailed discussion is given in the following section.

In general, the creep property depends on environmental conditions. Temperature-dependent creep compliance at 100 h is shown in Figure 7(a). For ARAMID and tensilized-type PET, creep compliance is relatively constant, whereas the creep
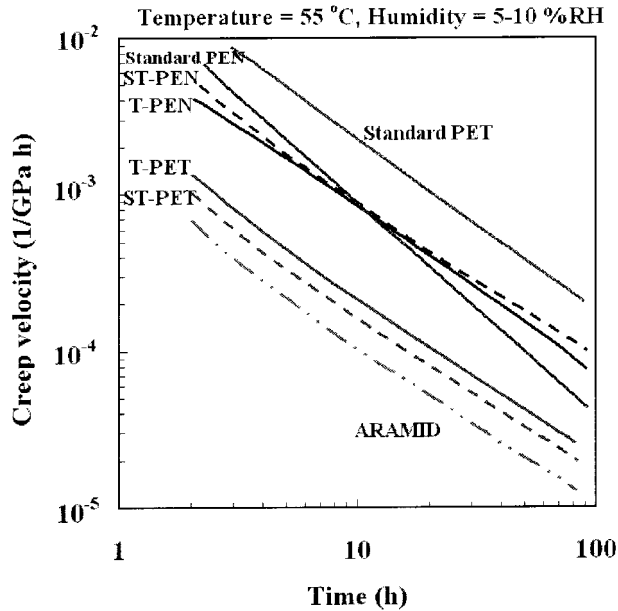
Figure 6 Creep-velocity measurements for polymeric films.

compliance for PEN and Standard PET increases with an increase in temperature. This means that PEN and Standard PET have more molecules with higher mobility at higher temperature in the temperature range used for magnetic tapes. To further quantify the viscoelastic behavior of polymeric films, the amount of lateral contraction due to Poisson effects can be calculated. Because magnetic tapes are placed under tension in a tape drive, any lateral contraction as well as any creep deformation associated with the applied external tension can occur. This contraction could lead to "read errors" if there is a mismatch between tracks on the tape and tracks on the head. Therefore, a minimal amount of lateral contraction is desirable if the polymeric film is used as a substrate for magnetic tapes.[1]

Calculated lateral contraction at 100 h is tabulated in Table IV. The amount of lateral contraction was calculated assuming a Poisson's ratio of 0.3 and an applied external stress of 7.0 MPa.[1,2] A Poisson's ratio of 0.3 has been shown to be a valid number for PET[1] and also a valid approximation for the other polymeric films.[2] As an example, the lowest lateral contraction for 55°C and 5–10% RH is about 0.02% for ARAMID, followed by about 0.04% for tensilized-type PET. On the other hand, PEN shows a larger contraction of about 0.05–0.06%. It is evident from the definition that lateral contraction depends on creep compliance. Ob-

tained lateral contractions are likely to correspond to the previous research[1,2] for PEN and thick Standard PET. The properties of creep and contraction under tension appear to have been improved for tensilized-type PET and ARAMID. Temperature-dependent lateral contraction at 100 h is shown in Figure 7(b). The trends are similar to temperature-dependent creep compli-
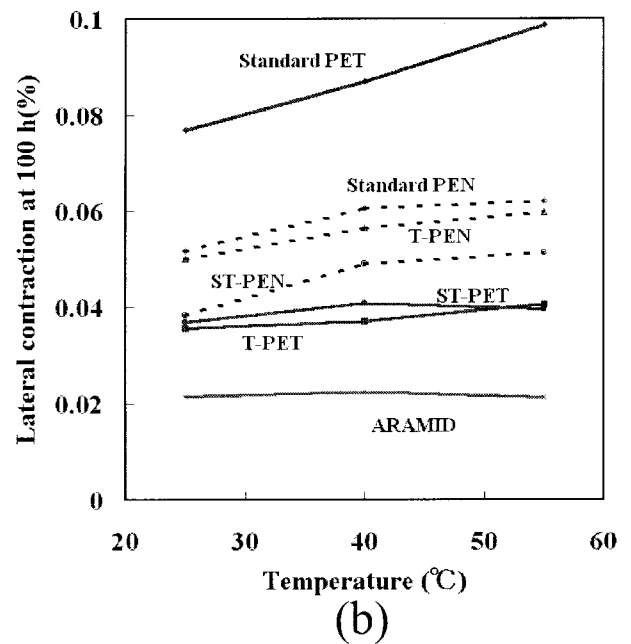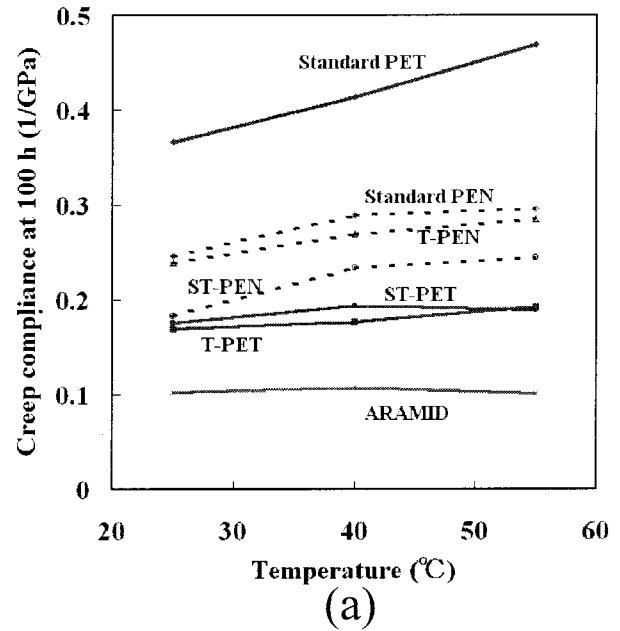

(a)

(b)

Figure 7 Temperature dependency of (a) creep compliance and (b) lateral contraction at 100 h.

Table IV   Lateral Contraction Under Some Environmental Conditions at 100 h

	Lateral contraction (%)[a]			
Sample	25°C 50–60%	40°C 15–25%	55°C 5–10%	55°C 80%
Standard PET	0.077	0.087	0.099	0.127
T-PET	0.036	0.037	0.041	0.055
ST-PET	0.037	0.041	0.040	0.040
Standard PEN	0.052	0.061	0.062	0.077
T-PEN	0.050	0.056	0.060	0.079
ST-PEN	0.038	0.049	0.051	0.072
ARAMID	0.021	0.022	0.021	0.023

[a] Calculations assuming Poisson's ratio of 0.3 and applied external stress of 7.0 MPa.

ance, and PEN and Standard PET have greatly larger contractions at higher temperature.

Creep-recovery Characteristics

At the end of a creep-compliance measurement, recovery experiments were performed. The creep deformation cannot be recovered immediately due to viscoelastic contribution. The recovery process is a time-dependent phenomenon that occurs at the identical rate with the original rate of creep. Figure 8 shows creep-recovery measurements at 55, 40, and 25°C. It is desirable that almost complete recovery experiments need about 10 times the period during which loads are applied.[8] In this study, however, recovery measurements were carried out for 10 h after removing the stress, and creep-recovery characteristics were predicted. Another reason is that it should be important to recover for a short period in a real magnetic tape. The residual strains at 10 h after removing the stress are tabulated as the amount of compliance in Table III.

After 100 h, the load is removed and the strain begins to recover. It can been seen that there is a rapid decrease in compliance that occurs almost immediately when the load is removed. This rapid decrease is indicative of the elastic and short-term viscoelastic behavior. The long-term viscoelastic behavior is measured for the next 10 h and occurs at the rate that should be equal (but opposite) to the rate of creep. The residual strains at 10 h are still less for ARAMID and tensilized-type PET than for PEN and Standard PET at all the temperature levels. Consequently, it can be predicted that ARAMID and tensilized-type PET are likely to be recovered almost completely. However, unlike ARAMID and tensilized-type PET, PEN and thick Standard PET have some residual

strains after 10 h of recovery. The existence of the residual strains could cause data on the magnetic tapes to be lost if the films are used as a substrate for magnetic tapes. To take an example at a 55°C temperature level, the residual compliance of $0.036 – 0.048$ GPa^{-1} for PEN means the residual strain of 0.025–0.034%, and the residual strain for Standard PET is approximately 0.1%. This behavior for thick-type PET was also observed in earlier work by Bhushan,[1] and it could be due to nonrecoverable or permanent deformation accumulated during creep. Under constant stress, the rate of strain approaches a limiting value, and a situation of steady-state flow is eventually attained, governed by the Newtonian viscosity. This steady-state flow can be regarded as a permanent deformation. In this respect, the creep velocity can be related to the reciprocal of viscosity or a nonrecoverable response.[1] As mentioned above, creep-velocity measurements show that ARAMID is the lowest, followed by tensilized-type PET, PEN, and Standard PET. This behavior is consistent with a nonrecoverable response. Furthermore, a permanent deformation is likely to be dependent on the temperature and be larger at a higher temperature level.

Creep-compliance Measurements Under High Humidity

The amount of creep compliance depends on environmental conditions. As mentioned above, the amount increases with an increase in temperature. This behavior is due to the high mobility of polymeric chains. In the same way, it is important to investigate the effect of humidity. The creep experiments under high humidity were made at 55°C and 80% RH, which is the upper-limit condition if the polymeric films are used as a sub-

strates for magnetic tapes. Figure 9 shows creep-compliance measurements for 55°C and 80% RH both on a linear scale and on a log–log scale. The data of creep compliance are tabulated in Table V.
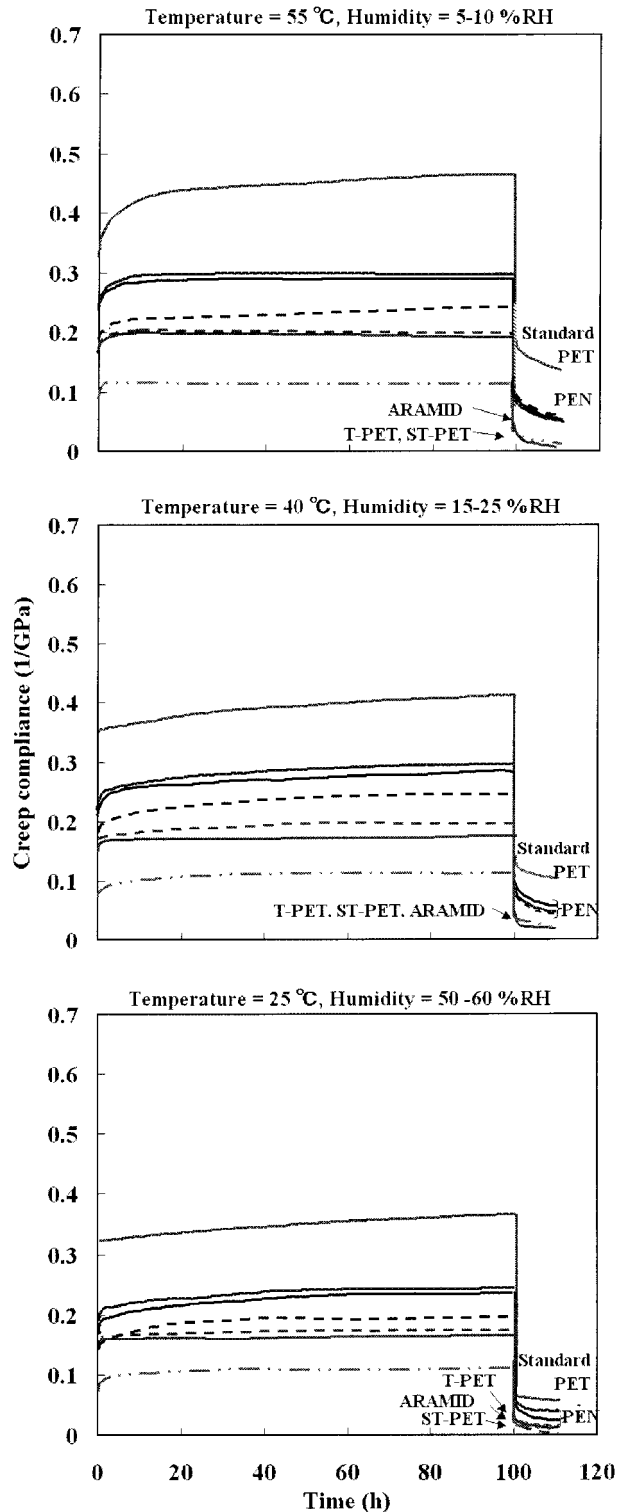

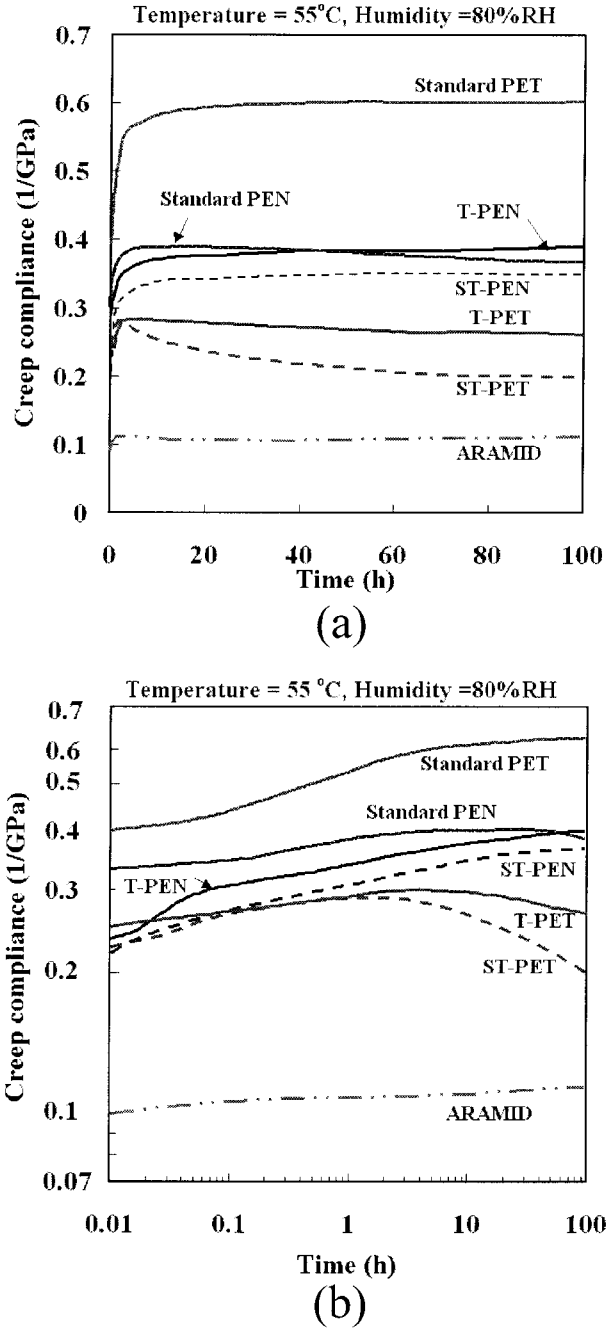Figure 8 Creep-recovery measurements for poly-meric films at 55, 40, and 25°C.

(a)

(b)

Figure 9 Creep-compliance measurements for poly-meric films at 55°C and 80% RH. Plotted on (a) linear axes and (b) log–log axes.

According to the measurements, ARAMID shows the lowest creep, followed by tensilized-type PET. It can be seen that PEN shows larger creep deformation. This behavior is analogous to the observations for 55°C and 5–10% RH. It should be noted that the amounts of creep compliance for 55°C and 80% RH is somewhat larger than those for 55°C and 5–10% RH for PET and

Table V   Creep Compliance at 55°C and 80% RH

Sample	Creep Compliance (1/GPa; 55°C, 80% RH)						
	0.01 h	0.1 h	1 h	10 h	100 h	110 h[a]	100 h − 0.01 h[b]
Standard PET	0.387	0.418	0.504	0.581	0.606	0.231	0.219
T-PET	0.241	0.253	0.277	0.285	0.261	0.014	0.020
ST-PET	0.218	0.256	0.278	0.259	0.191	−0.035	−0.027
Standard PEN	0.321	0.334	0.366	0.386	0.367	0.084	0.046
T-PEN	0.225	0.288	0.329	0.371	0.376	0.107	0.151
ST-PEN	0.201	0.259	0.295	0.334	0.344	0.113	0.143
ARAMID	0.098	0.104	0.109	0.108	0.111	0.020	0.013

[a] 10 h after removing external applied stress.
[b] Increment of creep compliance from 0.01 to 100 h.

PEN. Consequently, water molecules are likely to enter into polymeric molecules and cause higher mobility to polymeric chains. In other words, the effect of the higher-humidity condition is as much as an increase in temperature. This effect of humidity on PET and PEN films is shown schematically in Figure 10. Note that water molecules cannot enter into the crystalline region but can into the amorphous region in the polymer structure, since the amorphous region has a space where water molecules can be absorbed. Bhushan[1] presented that, at higher humidity, water vapor plasticizes the film, which lowers the glass transition temperature and increases creep. The effect is likely to be seen both in PET and PEN. It is interesting that ARAMID shows a low effect of high humidity. ARAMID contains amide groups, which have intermolecular hydrogen bonds. To take an example of polyamide, Nylon contains amide groups and the presence of moisture has a dramatic effect on the mechanical behavior.[8] This means that the absorbed water molecules reduce
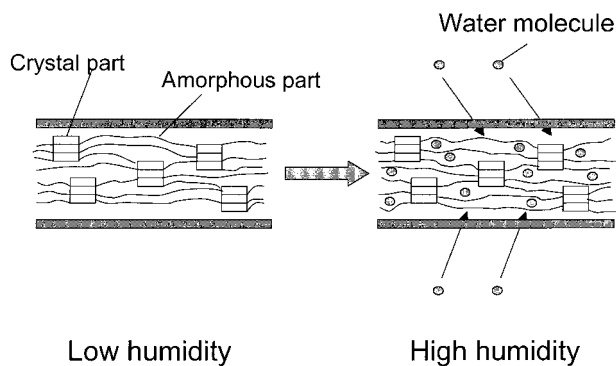
the effect of interchain hydrogen bonds. For ARAMID, however, the creep property is unlikely to be influenced by the water molecules. For this reason, it is highly probable that ARAMID consists of greatly rigid molecules and leads to higher packing and lower space.

Some reduction of creep compliance can be detected during the creep measurements of tensilized-type PET. This means that tensilized-type PET shows competitive behavior between creep deformation and shrinkage, although creep deformation could be the dominant factor. At the end of creep measurements, the load was removed and recovery tests were started. The results are shown in Figure 11. The largest residual strain after 10 h can be seen for Standard PET, followed by PEN, ARAMID, T-PET, and ST-PET. Basically, this trend appears to be similar to the results for 55°C and 5–10% RH. However, ST-PET exhibits slight shrinkage, which is negative compliance. On the other hand, PEN and Standard PET have still more residual strain, which is positive compliance.

As stated above, creep compliance is dependent on environmental conditions: temperature and humidity. Figure 12 summarizes creep compliance at 100 h. In general, higher temperature and higher humidity could cause the polymeric films to creep more. For ST-PET and ARAMID, the influence is very low. Creep deformation under all conditions is the largest for Standard PET, followed by PEN, tensilized-type PET, and ARAMID. For each sample, creep-compliance measurements at all the environmental conditions are shown in Figure 13. The results obtained for PEN and Standard PET is comparable with those obtained in the previous study.[1,2] The environmen-

Figure 10   Schematic showing effect of humidity on PET and PEN polymeric structure.
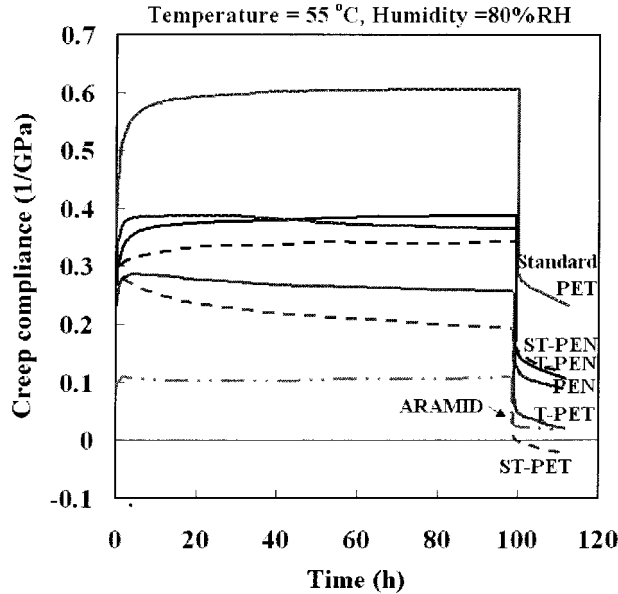
Figure 11 Creep-recovery measurements for polymeric films at 55°C and 80% RH.

tal stability on creep seems to be significantly larger for tensilized-type PET and ARAMID throughout the experiments, whereas PEN shows a greater effect of both temperature and humidity on creep. PET has somewhat greater effects of humidity on creep, because the condition of 55°C and 80% RH might have a similar increase in temperature close to glass transition temperature.

Prediction of Long-term Creep Behavior Using Time–Temperature Superposition

Based on the data of creep compliance, master curves were generated to predict long-term creep behavior at ambient temperature after several years. The analytical technique is known as time–temperature superposition.[1,8,10–12] Using this technique, creep measurements at the elevated temperatures shown in Figure 13 are superimposed on one another to predict the behavior at longer time periods. Creep deformation during storage at ambient temperature can be estimated. This analytical method is applied on the ground that most polymer materials will behave in the same manner at a particular high temperature, as they will when they are deformed on a long-time scale at a lower temperature. In other words, there is a correspondence between time (or rate of deformation) and temperature.

Results from the above analysis are presented in Figure 14(a) for the MD to predict the creep

compliance at 25°C as a reference temperature over 10^6 h (approximately 100 years). Creep experiments at a temperature higher than the 25°C reference temperature correspond to a longer time period. Therefore, the curves of 40 and 55°C were shifted to the right, and master curves were generated. The shift factors are tabulated in Table VI, and they show how much each curve was shifted to enable a smooth curve to be obtained. Shift factors are regarded as the interdependence of temperature and time (or strain rate). Note that shifting to the right corresponds to larger negative shift factors. Some vertical shifting is also necessary to accommodate differences in the initial elastic response when the film samples are loaded as well as differences in the elastic moduli at elevated temperature. However, this vertical shifting rarely exceeds 5% of the total creep compliance measured for a polymer.

According to master curves shown in Figure 14(a), ARAMID shows the lowest amounts of creep. It is clear that tensilized-type PET also shows considerably lower creep deformation. In contrast, PEN shows somewhat more creep at all time periods, and Standard PET has the largest amounts of creep. These observations were consistent with those at each temperature shown in Figure 5. The slopes of the curves in Figure 14(a) indicate the rate of creep or creep velocity. Creep-velocity measurements presented in Figure 6 show the results of the changes using the last decade of the creep data observed at 55°C. It is also useful to consider the overall slope of the master curve from 0.1 to 10^6 h. It should be noted that tensilized-type PET has the lowest rate of
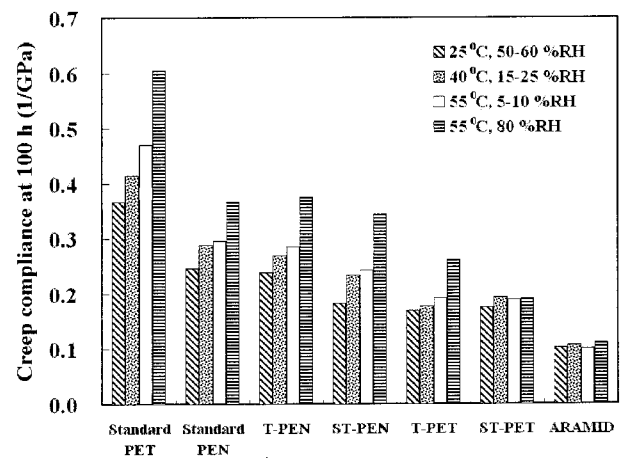

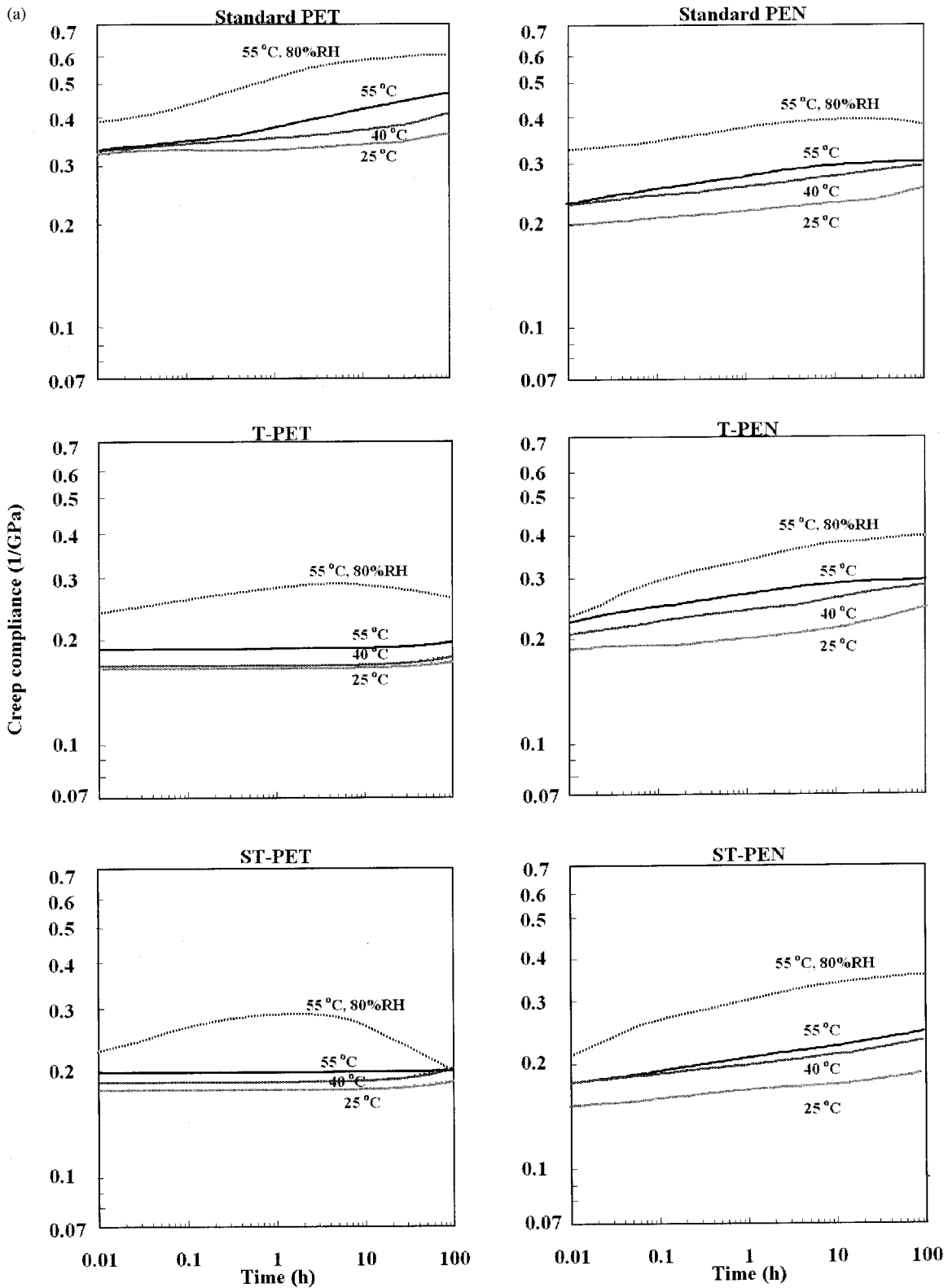**Figure 12** Summary of creep-compliance data at various environmental conditions.

Figure 13 Creep-compliance measurements at various environmental conditions: (a) PET and PEN; (b) ARAMID.
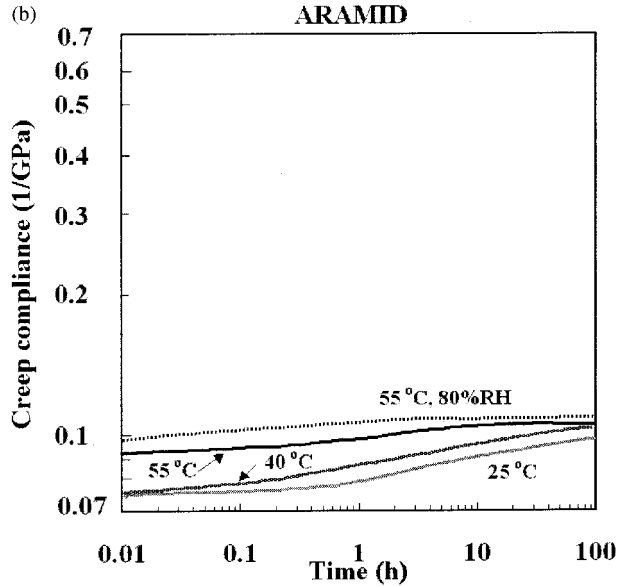
Figure 13 (*Continued*)

creep because the slopes of these master curves are relatively low. Although ARAMID has the lowest rate at 55°C, it can be seen that the initial part of the master curve has a slight slope because the creep velocity of ARAMID at 25 and 40°C is similar to that of PEN. However, the creep of ARAMID remains relatively constant at a longer time. On the other hand, PEN and Standard PET have a creep velocity that increases throughout the experiments.

The shift factors shown in Table VI were obtained for each temperature from the time–temperature superposition analysis. Using these shift factors, the value of any viscoelasitc property obtained at temperature T and time t can be related to the reference temperature T_r. For example, creep compliance is expressed in the following equation:[1,8,10,11]

$$D(t,T) = \frac{T_r\rho_r}{T\rho} D(t/a_T, T_r) \qquad (3)$$

where $D(t,T)$ is the creep compliance at time t and temperature T; a_T, the shift factors from the time–temperature superposition analysis; t/a_T, the reduced time from the time–temperature superposition master curve; T_r, the reference temperature from the time–temperature superposition analysis (in K); T, the experiment temperature corresponding to the shift factor (in K); ρ_r, the density of material at the reference tempera-

ture; and ρ, the density of the material at an experiment temperature corresponding to the shift factor. The temperatures and density ratios are due merely to thermal expansion. It is generally sufficient to approximate the ratio $T_r\rho_r/T\rho$ by the temperature ratio T_r/T, which corresponds to the vertical shift in generating the master curve.

The shift factors can be related to the apparent activation energy for the creep process, by assuming that the viscoelastic deformation process has an Arrhenius temperature dependence. The Arrhenius relationship shown below is very similar to the earlier form of the WLF equation[12] and is used to make this prediction for the so-called secondary relaxation or motion in the material[1,11]:

$$\log a_T = \frac{-\Delta H}{2.303R} \left(\frac{1}{T_r} - \frac{1}{T}\right) \qquad (4)$$

where ΔH is the activation energy in kJ/mol, and R, the universal gas constant (= 8.3145 J mol^{-1} K^{-1}).

Equation (4) is derived from the following assumed relationship for the retardation time; the retardation time is used in the following mathematical form based on a generalized Kelvin–Voigt model [2]:

$$\tau_k(T) = A_k\exp(\Delta H/RT) \qquad (5)$$

and

$$D(t,T) = D_0(T) + \sum_{k=1}^{k} D_k(T)\{1 - \exp[-t/\tau_k(T)]\}$$

$$(6)$$

where $\tau_k(T)$ is the discrete retardation times for each Kelvin–Voigt element at temperature T; A_k, a constant; $D_0(T)$, the instantaneous compliance at time $t = 0$ and temperature T; and $D_k(T)$, the discrete creep compliance terms for each Kelvin–Voigt element at temperature T. According to eq. (5), higher activation energy at a given temperature led to a higher retardation time, which, in turn, influences the lower magnitude of the delayed compliance, that is, the second term in eq. (6).[13] Thus, the activation energy ΔH should be interpreted as the energy required to activate the molecular process that causes creep.

The activation energy ΔH can be obtained by plotting $log\ a_T$ against $1/T$ and using linear regression to determine the slope of the straight
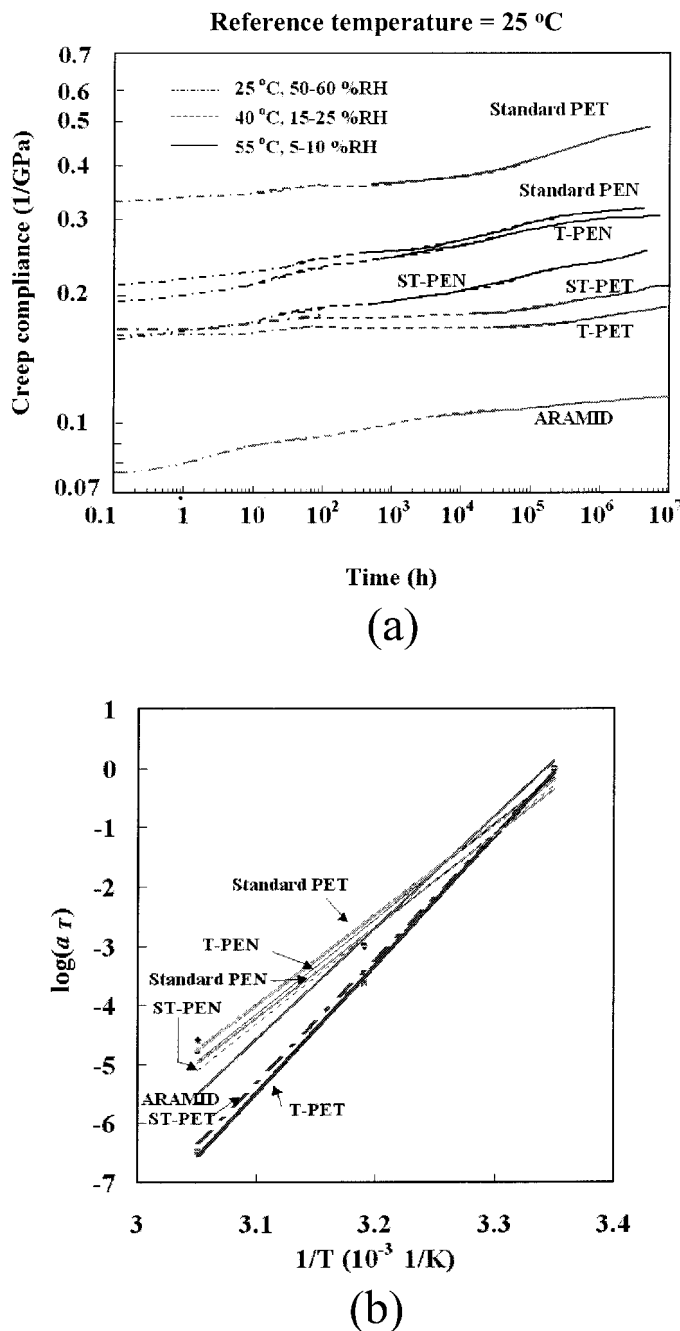
Figure 14 (a) Creep-compliance master curves at 25°C reference temperature for polymeric films. (b) Temperature dependence of shift factors, log a_T, obtained from time–temperature superposition.

line from eq. (4). Figure 14(b) shows the results of this analysis, and the obtained activation energy for each sample is tabulated in Table VI. The activation energy for tensilized-type PET of 400–410 kJ/mol is the largest. This result suggests that it is difficult for tensilized-type PET to undergo creep deformation, which is coincident with

the trends of master curves in Figure 14(a) and creep data in Figure 5. ARAMID has, likewise, a relatively larger activation energy of 360 kJ/mol. In contrast, PEN and Standard PET have significantly smaller activation energies of about 300–310 and 290 kJ/mol, respectively. These results mean that PEN and Standard PET are subjected

Table VI   Shift Factor and Activation Energy for Creep

Sample	Shift Factor log a_T		Activation Energy ΔH (kJ/mol)
	40°C	55°C	
Standard PET	−3.00	−4.58	290
T-PET	−3.65	−6.48	410
ST-PET	−3.70	−6.18	400
Standard PEN	−3.60	−4.60	300
T-PEN	−2.99	−4.79	310
ST-PEN	−3.48	−4.78	310
ARAMID	−2.60	−5.65	360

more to creep deformation. Bhushan,[1] in an earlier work, showed that the activation energy for the creep of PET is around 200–240 kJ/mol. Weick and Bhushan,[2] in a previous research, presented that the activation energy for PET, PEN, and ARAMID is about 310, 310, and 300 kJ/mol, respectively. They supposed that PET could be improved in processing. In this study, it is likely that the properties of PET, such as tensilized-type PET, are highly improved in advanced processing. Higher activation energy for ARAMID could also be due to an improvement in processing. In addition, the results of PEN and Standard PET are consistent with the previous research.[1,2]

A linear Arrhenius plot suggests that the molecular motions should be related to secondary relaxation. This is reasonably true for all the materials in Figure 14(b). Secondary relaxation is the motion in the glassy state below the glass transition temperature and should arise from localized motions. The motions can be distinguished from larger-scale motions to accompany the glass transition. Note that a nonlinear relationship between $log\ a_T$ and $1/T$ is usually fitted to the WLF equation,[12] which is typically valid for viscoelastic data acquired at a wider range of temperature through the glass transition temperature. In this study, the creep experiments were performed below the glass transition temperature for all the materials, and linear plots are valid. A detailed discussion on the secondary relaxation for each material will be presented in the following section.

Master curves were also generated to predict long-term creep behavior at a 5–10% RH level after several years. The analytical technique is known as time–humidity superposition,[1] similar to time–temperature superposition. Using this technique, creep measurements at elevated humidity at the same temperature level shown in Figure 13 are superimposed on one another to predict the behavior at longer time periods. The theory is on the same ground of time–temperature superposition. Results from the above analysis are presented in Figure 15 for the MD to predict the creep compliance at 55°C and 5–10% RH as the reference temperature and humidity over 10^6 h (approximately 100 years). The curves of 80% RH were shifted to the right and master curves were generated.

The lowest amount of creep is shown for ARAMID, followed by tensilized-type PET, PEN, and Standard PET. These predictions are almost similar to the master curve generated using time–temperature superposition shown Figure 14(a). As an example of a different trend, the large increment of creep for T-PEN and the reduction of creep for ST-PET can be obtained.

Shrinkage Measurements

Shrinkage data are presented in Figure 16 in both the MD and TD at a 55°C temperature level. For all the samples, shrinkage in the MD is larger than in the TD, because the MD is along with the tensilized direction. The shrinkage behavior can be directly related to the polymeric structure such as crystallinity and amorphous orientation. Shrinkage is a nonrecoverable deformation that can be attributed to the relaxation of oriented molecules in the amorphous regions of the films.[1,14–18] In other words, shrinkage arises from the disorientation (relaxation) of the oriented amorphous phase into a more random state and results in removal of the residual stresses formed during processing of the films. Note that the oriented molecules in the amorphous region can be distinguished from the highly oriented molecules
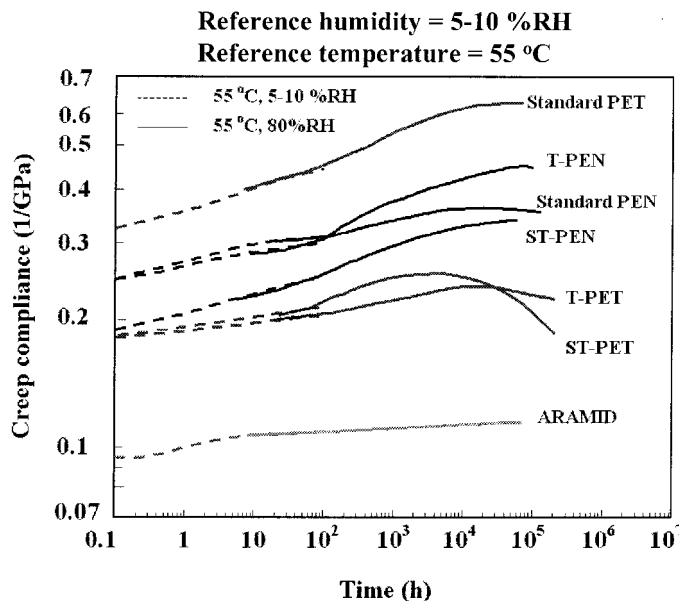
Reference humidity = 5-10 %RH
Reference temperature = 55 °C

Figure 15   Creep-compliance master curves at 55°C reference temperature for poly-meric films.

in the crystalline regions of the polymers. As a result, a total contraction of the films could occur in the orientation direction, and in this study, shrinkage seems to be larger in the MD along with the more oriented direction.

The different shrinkage property for each sample was observed in the MD. All the substrates shrank at 55°C. ARAMID shows the lowest shrinkage of about 0.02% at 100 h. Shrinkage for Standard PET is small due to short polymeric chains being stressed. T-PET shrinks by 0.07% and ST-PET shrinks by 0.06% at 100 h. On the other hand, the shrinkage of Standard PEN, T-PEN, and ST-PEN is 0.08, 0.07, and 0.04%, respectively. It is important to note that more tensilization appears to result in lower shrinkage for tensilized-type PET and PEN. The results can be accounted for by the glassy state below the glass transition temperature. This means that more tensilization would increase oriented elements and make the elements more resistance to shrinkage. Note that all the shrinkage measurements in the presented study were performed at 55°C, which is the upper-use limit for magnetic tape substrates. This temperature is in the glassy state below the glass transition temperature for all the materials. If the experiments are made above the glass transition temperature, more shrinkage would be obtained. As an example, heat shrinkage after 30 min at 105°C is shown in Table I. The temperature is above the glass tran-

sition temperature for PET. PET has more heat shrinkage at 105°C than reported in our measurements at 55°C and more tensilization leads to more shrinkage.

Relationship Between Dimensional Stability and Polymeric Structure

Creep behavior for the polymeric films can be related to the secondary relaxation or motion mentioned in the preceding section. The secondary motions involve the localized motion such as the so-called crankshaft mechanism and local-mode process, and distortion of the polymeric chains will occur through intermolecular distances.[11,19] These distances are determined by the type of intermolecular bonding. The secondary relaxation could occur in the amorphous regions, which have higher mobility than that of the crystalline regions. Note that the secondary relaxation can be distinguished from the most pronounced mechanical relaxation associated with the glass transition. In other words, the secondary relaxation results from motions in the glassy state below the glass transition temperature, and main polymeric chains are effectively frozen.[11,19] Thus, the secondary relaxation cannot be due to large-scale rearrangements of main chains. Even though the dimensional stability of the polymeric films is dependent mainly on the glass transition temperature, the secondary relaxation within the
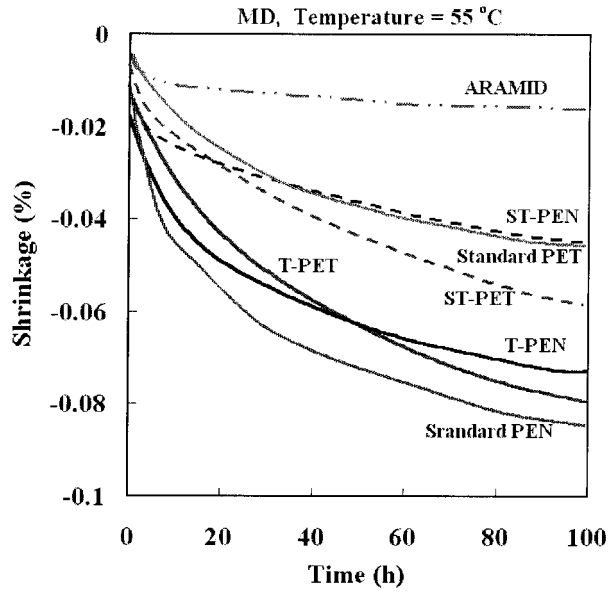
(a)
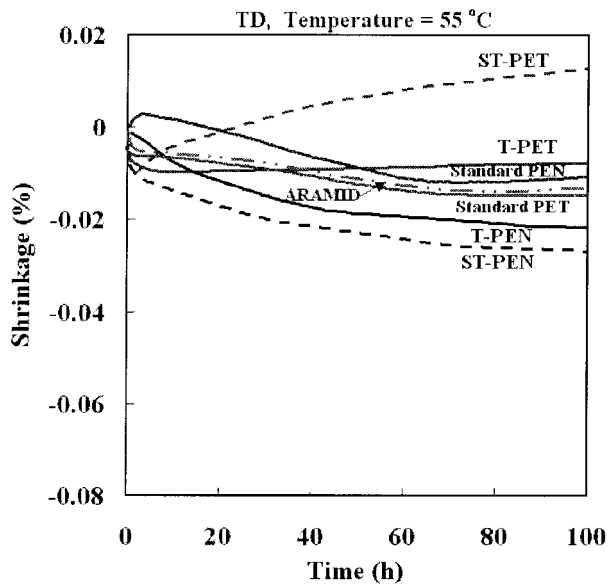
(b)

Figure 16 Shrinkage measurements for polymeric films in (a) MD and (b) TD.

Hindered rotation

Interlayer slippage

Figure 17 Schematics showing high mobility of naphthalene groups.

glassy state can have a significant effect on their viscoelastic response.

Dynamic methods such as the dynamic mechanical method and dielectric relaxation are widely applied to detect this glassy state relaxation.[11,19] In these methods, measurements over a temperature range at a constan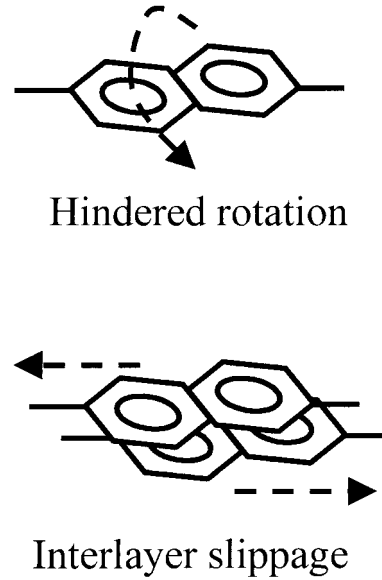t frequency are usually performed. For both PET and PEN, the low secondary relaxation, that is, β relaxation, can be detected at about -60 to $-40°C$ using dynamic methods. This β relaxation is attributed to motions of the ester (COO) groups or hindered rotation of methylene (CH_2) groups on the backbone of PET and PEN.[7,19–22] It is not probable that these motions contribute directly to creep behavior in this study, because the measured temperature range is different. In contrast, it is interesting that a prominent secondary relaxation, that is, β^* relaxation, could be seen at around $60°C$ only for PEN.[7,20–23] This presence dominates the dynamic response of PEN over a wide temperature range, -20 to $80°C$, and could substantially influence the viscoelastic response such as creep behavior at the corresponding temperature range. This relaxation can be related to the motions of the large and rigid naphthalene ring. One possible motion is hindered rotations of the naphthalene ring about the backbone.[20–23] Gillmor and Greener[7] suggested that another possible motion is interlayer slippage of the naphthalene ring. This behavior arises from stacked PEN molecules in order, such as liquid crystal parallel to the plane of the film due to the rigid and planar conformation of the naphthalene ring. The naphthalene groups with high mobility exhibited from ambient temperature to $60°C$ are shown schematically in Figure 17. This mechanism was also indicated in the processing of PEN film. Cakmak and Lee[24] suggested that, during

the deformation of PEN, the naphthalene rings are rapidly aligned parallel to the surface of the films and also occur at highly localized regions, which can lead to necking behavior during the deformation even above the glass transition temperature. Consequently, considerably larger creep compliance for PEN is responsible for the rotations or distortion of intermolecular bonding regarding naphthalene groups due to the secondary motions around 60°C. In addition, it should be noted that the existence of the β* process was observed at low frequency,[21] in which the viscoelastic response such as the creep property is predominant compared to the instantaneous elastic response.

The secondary relaxation for PET cannot be detected at temperature levels for the use of film as magnetic tapes. However, the molecules of Standard PET have higher mobility due to less oriented chains, and distortion of the intermolecular bonds such as van der Waals attractions could contribute to the largest creep process. Tensilized-type PET, which includes T-PET and ST-PET, is manufactured during high-drawing processing, and tensilized-type PET includes more oriented chains than does Standard PET. More oriented molecules with less mobility by nature lead to a lower creep process for tensilized-type PET. In contrast, PEN molecules have originally higher mobility within the temperature range for the use of films as magnetic tapes. Tensilization for PEN also results in less creep, but the contribution for PEN is less than for PET. In addition, PEN contains naphthalene groups, which inhibit crystallization due to a more complex stereochemical structure compared to the benzene ring for PET. Thus, PET has more crystalline and less amorphous regions than has PEN. Both PET and PEN could have less mobility in crystalline regions, and the amounts of amorphous parts are likely to influence the viscoelastic property such as creep. Cakmak and Wang[25] presented that the increase of crystallinity and orientation of chains in the amorphous region results in a reduction in creep strains for PET. Crystallinity as well as chain orientation play an important role in the determination of the creep property. The network structure formed by the crystalline regions significantly reduces the creep strains and strain rates by acting as an anchor to polymeric chains by entrapping them in higher-density and less mobile crystalline regions.

The secondary relaxation of ARAMID film Mictron[TM] has not been studied in detail. As an ex-

ample, however, other ARAMID or aliphatic polyamides, which contain amide groups, could be considered. One secondary relaxation is observed at −30 to 0°C for all the polyamides. This secondary relaxation, that is, β relaxation, is attributed to the motion of —NH$_2$ and —OH chain end groups, which is not involved in amide groups belonging to the intermolecular hydrogen bonds.[19,26] This relaxation is not observed at the temperature levels in this creep study. Another secondary relaxation can be detected at 140–170°C for aromatic polyamide such as poly(p-phenylene terephthalamide) (PPTA) fiber Kevlar® and poly(m-phenylene isophthalamide) fiber Nomex®. This secondary relaxation, that is, β* relaxation, is due mainly to hindered local motions of phenylene groups.[26,27] Similarly, this β* relaxation is predicted to be observed for the ARAMID film Mictron[TM]. However, this β* relaxation is also unlikely to be obtained at the temperature levels for the use of ARAMID film as an substrate of magnetic tapes. In addition, hydrogen bonds are the only weak link in the structure, but the hydrogen bonding in polyamide is inherently stronger than in polyester films. As a result, the total creep compliance tends to be lower for ARAMID film.

Shrinkage is associated mainly with the relaxation of the oriented amorphous chains and the removal of residual stresses formed during processing of the films.[1,14–18] Thus, shrinkage in the MD along with the tensilized direction is generally larger than in the TD. However, more tensilization is likely to lead to lower shrinkage for tensilized-type PET and PEN in the tensilized direction. The results suggest that more tensilization increases oriented elements and make the elements more resistance to shrinkage in the glassy state below the glass transition temperature. It is noted that shrinkage in this study could be distinguished from heat shrinkage above the glass transition temperature. As an example, heat shrinkage at 105°C, which is above the glass transition temperature for PET, is shown in Table I. The heat shrinkage is larger for PET than for PEN, and more tensilization leads to heat shrinkage. In addition, crystallinity plays an important role in the shrinkage property. As the crystallite formed during stress-induced crystallization in the drawing processing of a film increases, shrinkage is decreased.[28–30] Note that the crystallinity itself does not contribute to shrinkage behavior, although the increase of crystallinity leads to more resistance to shrinkage due to re-
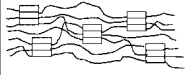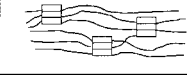
Substrates	Structure	Comments
Standard PET		• less oriented chains • larger fraction of crystalline structure
Tensilized-type PET		• more oriented chains • larger fraction of crystalline structure
PEN		• more oriented chains • smaller fraction of crystalline structure
ARAMID		more oriented chains (rigid units, hydrogen bonds)

Figure 18 Schematic of structures of various polymeric films.

duction of amorphous regions and a formed network structure. It is probable that highly oriented amorphous chains are similar to crystalline regions. Furthermore, a detailed morphology for ARAMID film is not known, but it is evident that ARAMID has a highly rigid chain and stronger intermolecular bonding such as hydrogen bonds. As a result, shrinkage could be the smallest for ARAMID.

A schematic of structures for polymeric films is summarized in Figure 18. Standard PET has less oriented chains and leads to the largest creep and less shrinkage. For tensilized-type PET, creep deformation is lower due to more oriented chains and a larger fraction crystalline structure. In contrast, PEN has a smaller fraction of the crystalline structure as well as higher mobility by nature on the basis of the existence of naphthalene groups and results in significant larger creep. The features for ARAMID are more oriented chains, rigid units, and hydrogen bonds. Consequently, ARAMID has the smallest creep and shrinkage.

CONCLUSIONS

Creep and shrinkage characteristics of improved ultrathin polymeric films were evaluated. These films include PET, which is currently the standard polymeric film used for magnetic tape substrates; thinner tensilized-type PET, PEN, and ARAMID have begun to be used for advanced magnetic tape substrates. Creep-compliance measurements for 100 h were preformed at 25, 40, and 55°C, which is the upper limit for magnetic tapes. In addition, creep compliance under a high humidity condition was also measured to investigate the effect of humidity on creep deformation.

Creep and creep-velocity measurements show that the alternative substrates, which include thinner tensilized-type PET, PEN, and ARAMID, tend to offer improvements over Standard PET. ARAMID shows the lowest creep deformation, creep velocity, and shrinkage, followed by tensilized-type PET and then PEN under all environmental conditions for use of magnetic tapes. Creep data acquired at 25, 40, and 55°C were used to predict the long-term creep behavior at ambient temperature using time–temperature superposition. The total creep compliance at long-term periods after several years is the lowest for ARAMID, followed by tensilized-type PET, PEN, and Standard PET. This observation is similar to creep-compliance data at each condition. Shift factors obtained from time–temperature superposition were used to predict the activation energy for the creep process. The linear slopes of Arrhenius plots in obtaining the activation energy suggest that the creep process can be related to the secondary relaxation or localized motions. The activation energy values are consistent with results of creep-compliance measurements, and the activation energy is larger for ARAMID and tensilized-type PET.

Secondary relaxation was discussed to explain a relationship between the polymeric structure and the dimensional stability. PEN has secondary relaxation associated with naphthalene groups at temperature levels for the use of magnetic tape substrates, and creep compliance could be considerably larger for PEN. Secondary relaxation does not exist at the same temperature levels for PET and ARAMID. In addition, smaller fractions of the crystalline structure influence the creep behavior for PEN, because the creep process could occur mainly in amorphous regions including elements with higher mobility. Tensilized-type PET has larger fractions of crystalline regions and more oriented chains with lower mobility and results in a lower creep process. ARAMID exhibits the lowest creep due to rigid chains and stronger intermolecular bonding such as hydrogen bonds.

Finally, shrinkage measurements were conducted at 55°C. Shrinkage arises from the relaxation of oriented chains, and shrinkage in the MD along with the tensilized direction is larger than in the TD. It is interesting that, in the tensilized direction, shrinkage also tends to be influenced by tensilization for both tensilized-type PET and PEN. More tensilization can lead to more resis-

tance to shrinkage in the glassy state below the glass transition temperature.

REFERENCES

1. Bhushan, B. Mechanics and Reliability of Flexible Magnetic Media, 2nd ed.; Springer-Verlag: New York, 2000.
2. Weick, B. L.; Bhushan, B. J Appl Polym Sci 1995, 58, 2381.
3. Weick, B. L.; Bhushan, B. IEEE Trans Mag 1995, 31, 2937.
4. Weick, B. L.; Bhushan, B. IEEE Trans Mag 1996, 32, 3319.
5. Weick, B. L.; Bhushan, B. J Info Stor Proc Syst 2000, 2, 207.
6. Weick, B. L.; Bhushan, B. J Appl Polym Sci 2001, 81, 1142.
7. Gillmor, J. R.; Greener, J. Proc Soc Plast Eng ANTEC97 1997, 1582.
8. Ward, I. M.; Hadley, D. W. An Introduction to the Mechanical Properties of Solid Polymers; Wiley: New York, 1993.
9. Tsou, A. H.; Greener, J.; Smith, G. D. Polymer 1995, 36, 949.
10. Ferry, J. D. Viscoelasitc Properties of Polymers, 3rd ed.; Wiley: New York, 1980.
11. Aklonis, J. J.; MacKnight, W. J. Introduction to Polymer Viscoelasticity; Wiley: New York, 1983.
12. Williams, M. L.; Landel, R. F.; Ferry, J. D. J Am Chem Soc 1955, 77, 3701.
13. Tschoegl, N. W. The Phenomenological Theory of Linear Viscoelastic Behavior: An Introduction; Springer-Verlag: New York, 1989.
14. Murthy, N. S.; Bednarczyk, C.; Rim, P. B.; Nelson C. J. J Appl Polym Sci 1997, 64, 1363.
15. Bhatt, G. M.; Bell, J. P. J Polym Sci Polym Phys 1976, 14, 575.
16. Willson, M. P. Polymer 1974, 15, 277.
17. Samuels, R. J. J Polym Sci A-2 1972, 10, 781.
18. Nobbs, J. H.; Bower, D. I.; Ward, I. M. Polymer 1976, 17, 25.
19. McCrum, N. G.; Read, B. E.; Williams, G. Anelastic and Dielectric Effects in Polymer Solids; Dover: New York, 1991.
20. Chen, D.; Zachmann, H. G. Polymer 1991, 32, 1612.
21. Ezquerra, T. A.; Balta-Calleja, F. J.; Zachmann, H. G. Acta Polym 1993, 44, 18.
22. Ahumada, O.; Ezquerra, T. A.; Nogales, A.; Blta-Calleja, F. J. Zachmann, H. G. Macromolecules 1996, 29, 5002.
23. Blundell, D. J.; Buckingham, K. A. Polymer 1985, 26, 1623.
24. Cakmak, M.; Lee, S. W. Polymer 1995, 36, 4039.
25. Cakmak, M.; Wang, Y. D. J Appl Polym Sci 1990, 41, 1867.
26. Frosini, V.; Butta, E. J Polym Sci B 1971, 9, 253.
27. Kunugi, T.; Watanabe, H.; Hashimoto, M. J Appl Polym Sci 1979, 24, 1039.
28. Mody, R.; Lofgren, E. A.; Jabarin, S. A. Proc Soc Plast Eng ANTEC2000 2000, 1695.
29. Mascia, L.; Fekkai, Z. Polymer 1993, 34, 1418.
30. Mascia, L.; Fekkai, Z.; Guerra, G.; Parravicini, L.; Auriemma, F. J Mater Sci 1994, 29, 3151.